INTEGRIN AND CYTOKINE SIGNALING IN MYOFIBROBLAST DIFFERENTIATION: A NETWORK MODELING APPROACH

By

Alison Koelle Schroer

Thesis

Submitted to the Faculty of the

Graduate School of Vanderbilt University

in partial fulfillment of the requirements

for the degree of

MASTER OF SCIENCE

in

Biomedical Engineering

May, 2014

Nashville, Tennessee

Approved by:

W. David Merryman, Ph.D.

John P. Wikswo, Ph.D.

ACKNOWLEDGEMENTS

First, I would like to thank Dr. David Merryman for his guidance and support throughout the last three years. Second, I would like to thank my fellow lab members, especially Larisa Ryzhova. Third, this work was funded by the National Science Foundation Career Award to WDM (1055384) and Graduate Research Fellowship to AKS (DGE-0909667) and the NIH (HL094707).

TABLE OF CONTENTS

LIST OF TABLES

LIST OF FIGURES

Figure Page

CHAPTER I

INTRODUCTION

Background

Fibrotic disease

Connective tissue fibrosis can occur in many tissue and organ systems and is a significant cause of morbidity and mortality in American society. As the population ages, fibrotic diseases such as athlerosclerosis, interstitial lung disease, glomerulosclerosis and heart valve disease will likely increase in prevalence. Cardiac hypertrophy and scarring after myocardial infarction are examples of deadly fibrotic diseases with a large effect on our population. All of these diseases are characterized by an accumulation of extracellular matrix (ECM) proteins, notably type-1 collagen, and a loss of tissue compliance, both of which can severely impair organ function.[1] Resident fibroblast cells are responsible for producing and maintaining connective tissue and are a prime suspect in the development of fibrotic pathologies. These cells can differentiate into the active myofibroblastic phenotype in response to environmental cues, and demonstrate enhanced contractility and heightened ECM production, both of which are important for normal development and wound healing (Figure 1). However, if the cells fail to return to the quiescent fibroblast phenotype, excessive connective tissue accumulation and stiffening can occur, leading to the activation of neighboring cells and the development of chronic tissue fibrosis.[2] Two major factors which promote myofibroblast differentiation are mechanical stiffness and transforming growth factor beta 1 (TGF-β1).[3] TGF-β1 is a potent stimulator of myofibroblast differentiation that is critical during normal development, but it also can contribute to the development of fibrotic disease. Fibroblast growth factor (FGF) opposes TGF-β1 signaling during development and disease and promotes the quiescent fibroblast

phenotype.[4-5] Understanding the processes by which myofibroblast activation occurs is especially crucial to the treatment of connective tissue diseases among infants and the elderly.

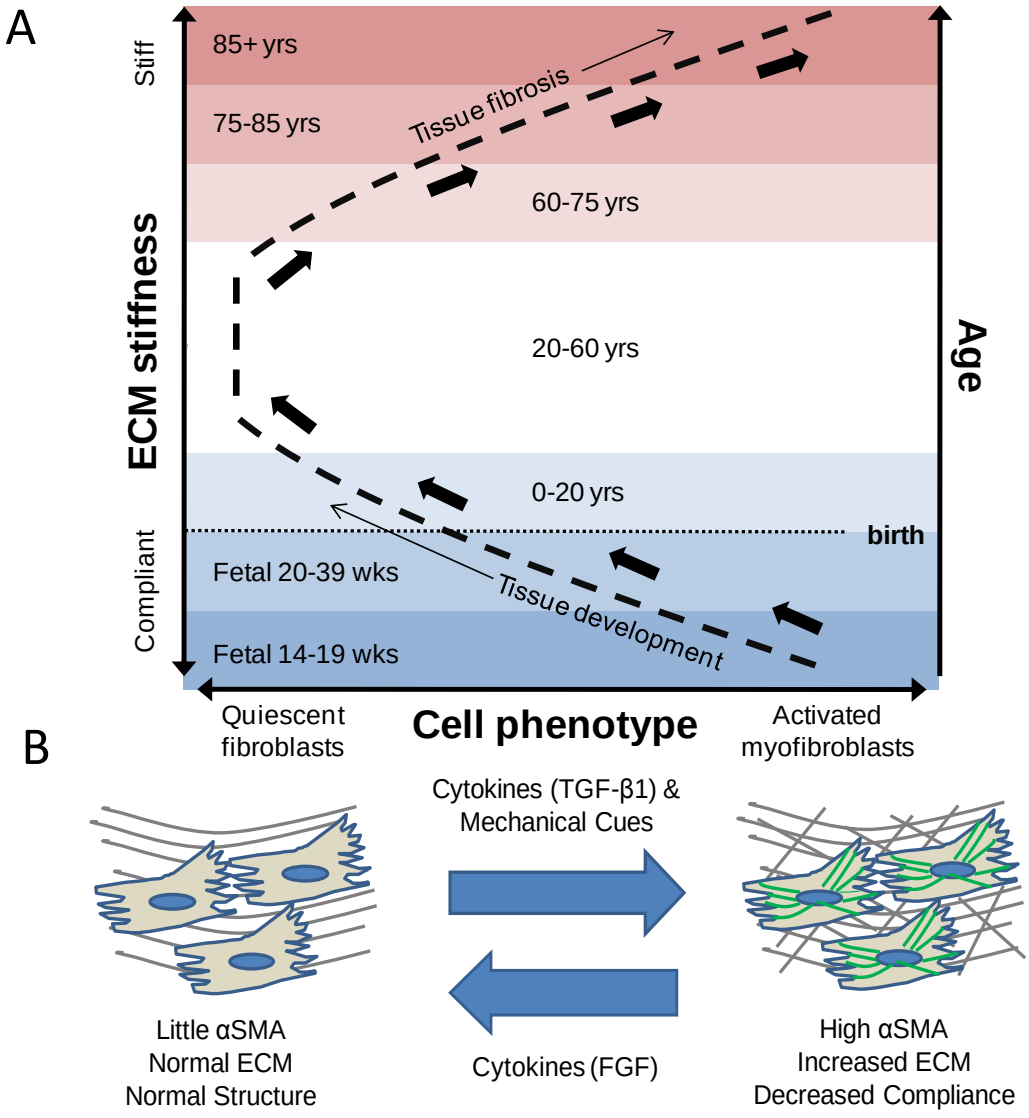

Figure 1: Fibroblast phenotypic changes with age, ECM stiffness and chemical cues. Fibroblast cells are highly activated during development and old age, life stages correlated with significant changes in ECM stiffness and structure. In addition to mechanical triggers, growth factors TGF-β1 and FGF are present during development and old age and regulate cell phenotype and the tissue characteristics associated with tissue fibrosis.

Integrins in mechanotransduction

Mechanical stress and strain are known to cause myofibroblast differentiation during both development and old age. An important way cells experience their mechanical environment is via integrin-mediated signaling pathways (Figure 2). In addition to their role as a structural protein, integrins can sense mechanical tension and increased substrate rigidity, which leads to phosphorylation of intracellular signaling molecules, including the tyrosine kinase Src,[6] focal adhesion kinase (FAK),[7] and the downstream mitogen-activated protein kinase (MAPK) p38.[8] There are many specific isoforms of integrins which recognize a host of ECM proteins and transduce signals to intracellular kinases in a process known as outside-in signaling.[9] Diversity in the cytoplasmic tail of different β subunits determines the intracellular connections of these molecules.[10] The β1 isoform is found in collagen and fibronectin-specific integrin receptors and has been shown to enhance FAK autophosphorylation on tyrosine 397.[7] The β3 isoform has been shown to physically interact with Src and enhances Src activation.[11-12] Integrins can also experience inside-out signaling, by which intracellular kinases and enzymes can modify the intracellular domain of integrin subunits to activate integrins and allow for stronger adhesions to the ECM[13] and ECM remodeling.[14-15] Both Src and FAK are involved in the maintenance and turnover of focal adhesions that mechanically link integrins to the actin cytoskeleton.[9,14] The dual and complex role of integrins, FAK, and Src in structural and biochemical systems makes an integrated biophysical and biochemical approach extremely useful in clarifying this process.

Table 1: Glossary of Terms

Term	Description
αSMA	Alpha smooth muscle actin: myofibroblast marker
TGF-β1	Transforming growth factor beta 1
TβR2	Type II TGF-β1 Receptor
FGF	Fibroblast growth factor
FAK	Focal adhesion kinase
ERK	Extracellular signaling-related kinase
Src	Tyrosine kinase found in focal adhesions
MAPK	Mitogen-activated protein kinase
p38	MAPK involved in non-canonical TGF-β1 signaling
MEF+/+	Wild type mouse embryonic fibroblasts (MEFs)
FAK-/-	FAK null MEFs
SYF-/-	MEFs lacking Src, Yes, and Fyn, three Src family kinases

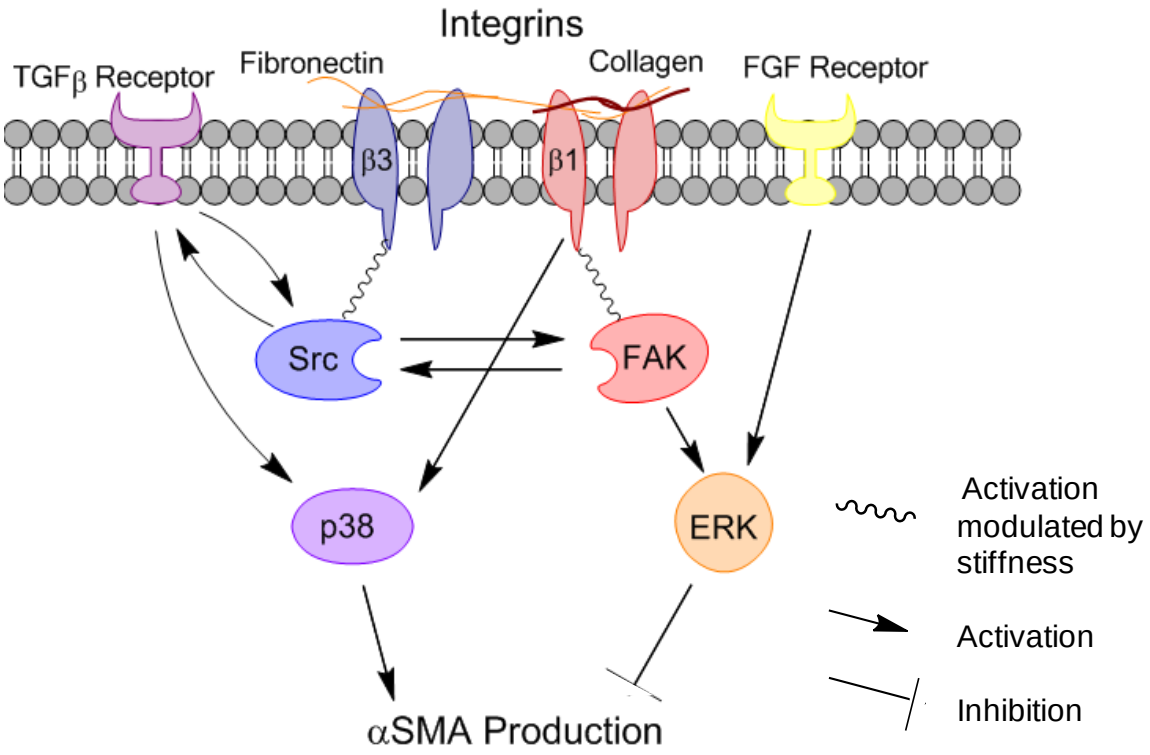

Figure 2: Schematic of relevant cell signaling network. The cartoon depicts the major pathways of activation and convergence on p38 and ERK kinases. Degredation and interactions details are not shown for the sake of clarity

Details of Src/FAK interaction

Src and FAK are both primed for activation by integrin engagement and focal adhesion formation, but there are complex, multistep interactions between these two kinases that affect their activation states. FAK is a large scaffolding protein that interacts with a host of other proteins and has several phosphorylation sites.[16] Autophosphorylation of tyrosine 397, which occurs after β1 integrin engagement, allows for association of the SH2 domain of the Src. This physical association promotes the open conformation of Src, which limits inhibitory phosphorylation of Src tyrosine 527 and allows for more phosphorylation of tyrosine 416, causing a significant increase in Src kinase activity.[17] With both enhanced kinase activity and close proximity, Src phosphorylates FAK at tyrosines 576, 577, 861, 925, and others.[16] This secondary phosphorylation activates the kinase activity of FAK and enhances signaling to downstream targets like ERK and p38.[18] It also allows for FAK autophosphorlyation of tyrosine 397 of surrounding FAK proteins.[16] One of the effects of Src/FAK downstream signaling is recruitment of csk to focal adhesions, which phosphorylates Src tyrosine 527 and limits Src activity, forming a negative feedback loop.[12,17]

TGF-β1 signaling promotes myofibroblast differentiation through Src and p38

In addition to its role in focal adhesion maintenance, Src is required for non-canonical TGF-β1 signaling to p38.[19] TGF-β1 binding to its type 1 receptor activates Src, which in turn phosphorylates tyrosine 294 on TGFβ receptor 2 (TβR2), leading to p38 phosphorylation.[20] This signaling is crucial for myofibroblast differentiation of aortic valve interstitial cells and other fibroblast cell types.[21] Mouse embryonic fibroblasts which cannot express Src family kinases (SYF-/-) have been shown to express significantly fewer myofibroblast markers than their wild type counterparts (MEF+/+) (Figure 3A). MAPK p38 is also critically important for myofibroblast differentiation.[21-22] Inhibiting p38 effectively blocks TGF-β1 induced myofibroblast differentiation,

but does not interfere with canonical smad signaling (Figure 3B). Within the nucleus, transcription factors MKL1 and SRF (downstream of Src and p38) are required for the transcription of αSMA and other markers of contractile myofibroblasts.[23]

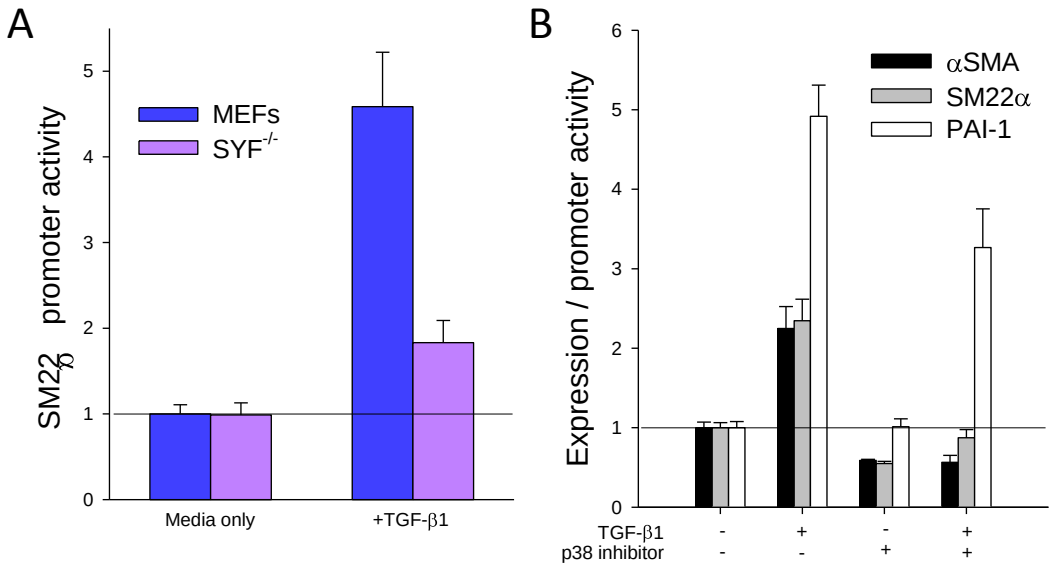

Figure 3: Src and p38 are necessary for TGF-β1 induced myofibroblast differentiation *Figure from Hutcheson* [21]

FGF signaling opposes myofibroblast differentiation

FGF is another factor that is critical for development and can have a potent effect on fibroblast phenotype. FGF signaling to ERK has been shown to prevent myofibroblast differentiation in MEFs and reverse TGF-β1 induced αSMA expression.[5,24] Kawai-Kowasa et al. demonstrated that expression of the transcription factor SRF is crucial for αSMA expression, but its function is blocked by phosphorylated ERK after FGF treatment (Figure 4).[5] Greenberg et al. found that this effect is modulated by FAK and does not occur in FAK-/- cells.[24] More study is needed to determine how ERK prevents αSMA expression during FGF signaling but is also activated by TGF-β1 signaling. FGF is also known to activate p38, a crucial player in TGF-β1

induced myofibroblast differentiation.[25] Understanding the crosstalk between MAPK signaling from TGF-β1 and FGF will clarify the intracellular signals governing myofibroblast differentiation.

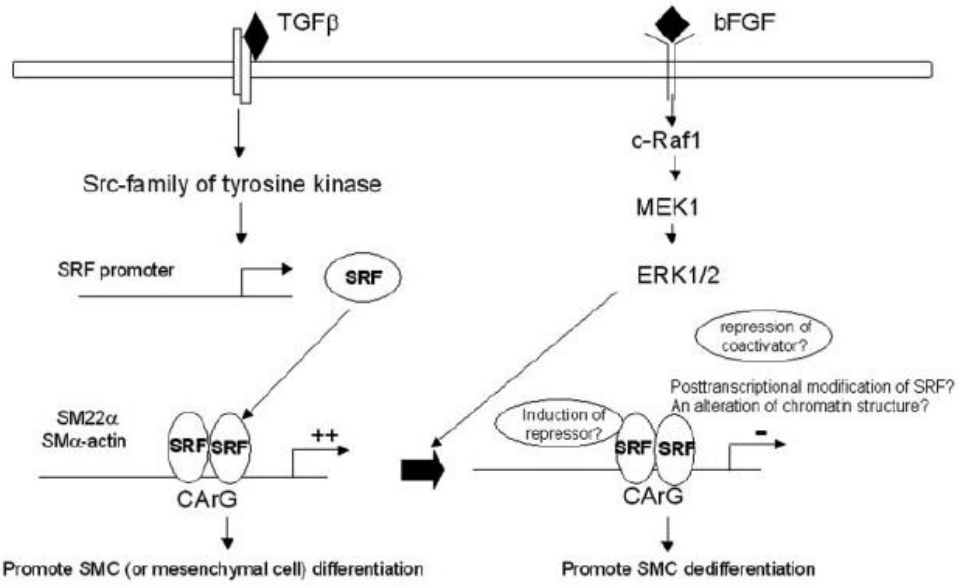

Figure 4: Proposed model of roles for Src and ERK in TGF-β1 and FGF regulation of differentiation. *Figure from Kawai-Kowasa*[5]

Utility of computational models of signaling networks

Computational models of cell signaling networks can be a powerful tool for analyzing and characterizing the complex interactions between intracellular kinases. Several models of parts of this system focus on integrin signaling through Src, FAK, and ERK,[26] the details of Src/FAK interactions,[27] TGF-β signaling,[28] and intracellular signaling to p38,[29-30] however, none address the crosstalk between integrin and growth factor signaling in the context of myofibroblast differentiation. Many computational models of cell signaling pathways take advantage of published values for rate coefficients for specific protein interactions.[26,29-30] A particular challenge of building network models is the dramatic increase in system complexity relative to single pathway models. Often, it is necessary to simplify a system for the sake of model tractability. In this case, modified reaction parameters must be estimated from

experimental data. Some models rely entirely on a large set of quantitative data to develop the model and its parameters.[31] However, when only a limited supply of reliable rate constants and quantitative data is available, trustworthy models have been developed which rely on a combination of previously reported and newly determined reaction constants.[32]

Objective

The objective of this work was to elucidate the roles of Src and FAK in the integrin and cytokine signaling that controls myofibroblast differentiation using a computational model capable of reflecting the relevant signaling events. Furthermore, this work aimed to study the dynamics of MAPK signaling, specifically p38 and ERK, in response to growth factor treatment and integrin signaling on surfaces with differing stiffness. The intent of the model was to compare the likely validity of different hypotheses about the nature of myofibroblast regulation.

Specific Aims

1. Determine how integrin transduction of mechanical stiffness activates Src and FAK to regulate myofibroblast differentiation
2. Develop computational models which describe the kinetics of the system
3. Determine the dynamic signaling events of TGF-β1 and FGF

CHAPTER II

MANUSCRIPT: DEVELOPMENT OF A COMPUTATIONAL MODEL OF MYOFIBROBLAST DIFFERENTIATION

Abstract

Fibrotic disease is a major cause of morbidity and mortality, and is characterized by the transition of resident fibroblast cells into the active myofibroblast phenotype. Alpha smooth muscle actin (αSMA) is a primary indicator of the myofibroblast phenotype, and is regulated by transforming growth factor beta 1 (TGF-β1), fibroblast growth factor (FGF) and substrate stiffness. Integrin signaling through Src and FAK converges with growth factor signaling and both signal through p38 and extracellular signal-related kinase 1 and 2 (ERK) to regulate αSMA production. While details are known about individual pathways, little is known about their interactions. To this end, an ODE-based model of this cell signaling network was developed in parallel with *in vitro* experiments to analyze potential mechanisms of crosstalk and regulation of αSMA production. We found that cells lacking Src produce significantly less αSMA than wild type cells, while cells lacking FAK produce significantly more. Increases in substrate stiffness and increasing TGF-β1 concentration cause significant increases in αSMA, while FGF causes a dose dependent decrease in αSMA. Western blot analysis revealed that TGF-β1 induces a gradual increase in ERK phosphorylation and a significant and sustained activation of p38. FGF stimulates a rapid, but transient activation of p38, and a much more dramatic and sustained activation of ERK. Our model effectively recreated αSMA expression levels across a set of 22 experimental conditions and matched transient phosphorylation of ERK and p38. These results support a potential mechanism for regulation of fibroblast differentiation: αSMA production is promoted by active p38 and Src and opposed by ERK.

Introduction

Fibroblast cells play a key role in producing and maintaining connective tissue throughout the body. The ability of these cells to differentiate into active myofibroblasts is important during development and wound healing, but prolonged myofibroblast activation can lead to overproduction of extracellular matrix proteins and stiffening of the surrounding tissue. While a critical step in scar formation during wound healing, this stiffening can cause heightened differentiation of neighboring fibroblasts through force transduction pathways and can lead to detrimental fibrotic pathologies in many organ systems.[2] One hallmark of the myofibroblast phenotype is the production of alpha smooth muscle actin (αSMA) stress fibers, which transmit intracellular forces and increase the contractility of the cells and surrounding tissue.[2,33] Clarifying the inputs and intracellular mechanisms which govern myofibroblast differentiation will provide insights into the pathophysiology of many fibrotic diseases.

Mechanical stress and transforming growth factor beta 1 (TGF-β1) are known to promote the myofibroblast phenotype,[2] and fibroblast growth factor (FGF) has been shown to promote the quiescent fibroblast phenotype,[5] but the intracellular effectors of these environmental cues have significant crosstalk,[34-35] as seen in Figure 5. Cells can experience mechanical tension and substrate rigidity through integrins, which are trans-membrane proteins that transduce forces from the ECM to intracellular structures like focal adhesions and stress fibers. Different isoforms of integrin subunits are activated to transmit mechanical signals by specific ECM proteins. Integrins with β3 subunits are activated by fibronectin and transmit mechanical signals through the tyrosine kinase Src.[6,16] Src and β3 integrin together enhance TGF-β1 non-canonical signaling to p38.[20,36-37] β1 integrin subunits activate focal adhesion kinase (FAK) in a stiffness-dependent manner.[7] Src and FAK are important in the formation and maintenance of focal adhesions and are known to form a complex and activate each other's kinase activity to enhance downstream signaling.[16,38]

Signaling through integrins and growth factors appears to converge at the intracellular level on two particular kinases, p38 and ERK. TGF-β1 signaling and β1 integrin signaling both activate p38, which has been shown to promote the myofibroblast phenotype.[8,39] Conversely, ERK is required for FGF inductiona of the quiescent fibroblast phenotype.[40] FAK serves as a docking site for Src and enhances Src activation and signaling to p38,[19] while transducing signals from integrins and FGF to enhance ERK activation and limit αSMA production.[24,41] FGF and TGF-β1 stimulate both p38 and ERK; however, they are known to lead to divergent outcomes,[5,42] as suggested by Fig 4A. The complex and dynamic interactions of these signaling pathways complicate the regulation of fibroblast differentiation.

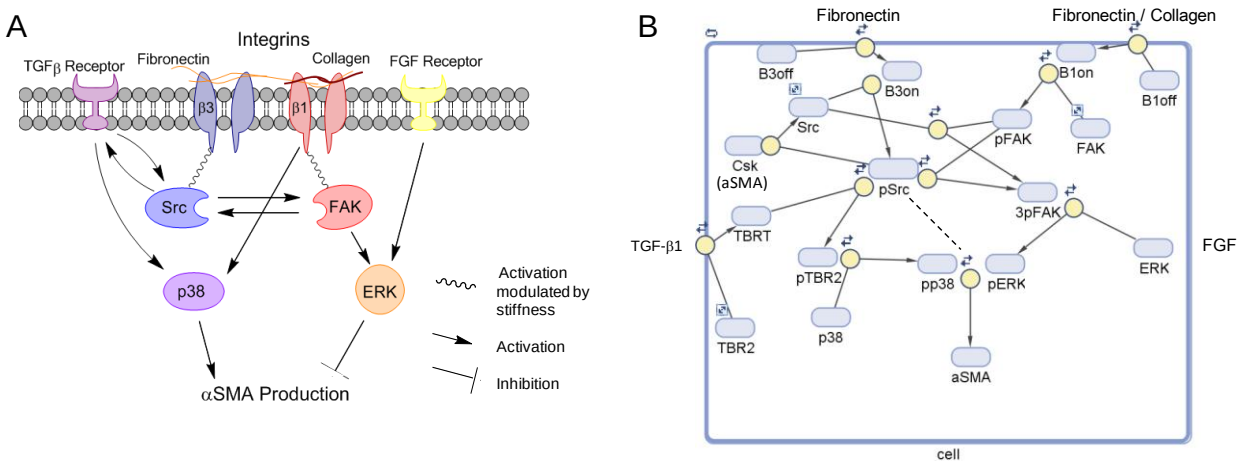

Figure 5: Relevant signaling network. A. The cartoon depicts the major pathways of myofibroblast regulation and convergence on p38 and ERK kinases. Degradation and interactions details are not shown for the sake of clarity. B. The schematic shows the model protein species and reactions. Proximity to the yellow node indicates that the rate of the reaction depends on the activation of the upstream protein species. The dashed line represents a direct contribution of Src to regulation of αSMA production.

Computational models of cell signaling networks have been developed and used in many biological systems to clarify complex interactions, especially when intracellular activation states are difficult to quantify.[43] Some models have been developed for subsets of this system to clarify specific mechanisms, but do little to address network effects and responses.[26-28] Modeling biological networks is challenging due to the high number of interactions, the range of

relevant time scales, and the difficulty of acquiring quantitative data of intracellular kinetics. Despite these hurdles, many model strategies have been developed and successfully implemented in similar network settings.[43] A model developed by Janes et al. integrates complex cytokine signals to predict apoptosis, and they countered these difficulties by focusing on data-derived models.[31] Further analysis of the same model indicated that the dynamic range of a given intracellular signaling event is more important for system function than the signal strength, which lessens the need to define system components with absolute protein numbers or concentrations.[44]

The goals of this work are to clarify the roles of FAK and Src in linking integrin and cytokine signaling, characterize the signaling profiles of TGF-β1 and FGF through p38 and ERK in the regulation of αSMA, and develop a quantitative model to evaluate and compare potential mechanisms for protein interactions in the regulation of myofibroblast differentiation.

In this study, we developed a computational network model to clarify the complex crosstalk between TGF-β1, FGF, and integrin signaling regulating the differentiation of fibroblasts. Known TGF-β1, FGF, and integrin signaling to p38 and ERK through Src and FAK from previously reported literature informed the development of an ODE-based model of fibroblast differentiation in different chemical and mechanical environments. The model was refined by fitting to experimental results for αSMA production and dynamic phosphorylation events. Sensitivity analysis and two model comparison techniques were developed to evaluate different model hypotheses and delineate potential mechanisms.

Materials and Methods

Cell culture

Wild type mouse embryonic fibroblasts (MEF+/+), MEFs lacking Src, Yes and Fyn (SYF-/-), and MEFs lacking FAK (FAK-/-)[45] were used in this study. Cells were cultured in DMEM supplemented with 10% FBS, 1% antibiotic-antimicrobial and 1% non-essential amino acids. Unless otherwise noted, cells were plated at a density of 8000 cells/cm^2 on tissue culture plastic (TCP) and kept in serum-free conditions during treatment with 1 ng/ml TGF-β1 or 10 ng/ml FGF.

PDMS for stiffness studies

Polydimethylsiloxane (PDMS) (Sylgard 184 from Dow Corning) culture surfaces were made with 10:1:0, 10:1:5, and 20:1:2 ratios of silicone-elastomer base to elastomer curing reagent to silicone oil as previously described.[46-47] Bulk stiffness of these formulations was measured to be 2.1, 0.9 and 0.24 MPa, respectively.[47] The dishes were then sterilized under UV light for 40 minutes and coated with human full-length fibronectin in filtered carbonate-bicarbonate buffer overnight to ensure proper cell adhesion.

Immunohistochemistry

Coverslips were coated in fibronectin by overnight incubation in a 50 μg/ml solution in sterile carbonate-bicarbonate buffer and rinsed in PBS before addition of cells. After 24 hours of treatment, cells were fixed with 4% paraformaldehyde and permeabilized in 0.4% triton, blocked in 1% BSA, and stained with a Cy3 conjugated monoclonal αSMA antibody (sigma). Slides were mounted in ProLong gold with DAPI mounting media to stain the nuclei and imaged at 20x magnification.

Quantification of αSMA production by indirect ELISA

Indirect ELISA assays with αSMA polyclonal antibody (Abcam) were used to quantify αSMA expression after 24 hours in serum-free conditions as previously described.[21]

Quantification of MAPK activation by western blot

Western blots were used to study dynamics of MAPK activation in MEF+/+ and FAK-/- cells as previously described.[21] Briefly, cells were serum-starved for 3-4 hours before treatment, and were lysed and diluted to equal protein concentration in RIPA buffer supplemented with protease and phosphatase inhibitors. Relative p38 and ERK phosphorylation was quantified by densitometry analysis and normalized to a loading control (β-actin, total ERK, or total p38) (cell signaling antibodies) and then to the average MEF+/+ no treatment case within each time point for each experiment.

Statistical analysis

For all experiments measuring outputs across a range of cell types and treatments, a two-way ANOVA was run within each time point to determine significant effects of cell type and treatment, and interactions between the two. The Holms-Sidak method and individual student t-tests with an overall significance level of 0.05 were used for multiple comparisons within cell-type and treatment groups. One-way ANOVA was used for dose response experiments which were limited to one cell type. Non-parametric tests (ANOVA on ranks or rank sum tests) were used if the samples failed the Shapiro-Wilks normality test or had unequal variance ($p < 0.05$).

Model development

The model is a system of ODEs describing the dynamics of relative protein activation and αSMA production in fibroblasts. To simplify the model, a normalized closed system was assumed, wherein the total amount of each protein species in the signaling pathway is

conserved at a value of 1. While many of these proteins have multiple phosphorylation states and conformations which affect their enzyme activity, most protein species were simplified to 2 activation states, “on” or “off”. Src, FAK, and TβR2 were given 3 activation states to capture more system interactions. In total, the model contains nine active variables (Table 2), 27 kinetic rate coefficients (Table 3), and 12 inputs and boundary conditions which can be varied experimentally and *in silico.* Figure 5B shows a general descriptive schematic of the interactions and protein species represented in the model. First order activation rates proportional to the relative activation of the upstream species were used to model signaling cascades, unless more specific interactions were known. Michaelis-Menten kinetics was used in cases of direct phosphorylation, as with Src activation of FAK tyrosines in the 400-900 range and Src phosphorylation of TGFβ receptor 2 (TβR2). A more detailed description of model formulation can be found in Appendix A.

Table 2: List of active variables

Variable name	Description
B1on	amount of activated β1 integrin as a fraction of total
B3on	amount of activated β3 integrin as a fraction of total
TBRT	TGF-β1 receptor (TβR2) with TGF-β1 ligand attached
pTBR2	phosphorylated and ligand bound TGF-β1 receptor (TβR2)
pS	activated Src kinase
pFAK	FAK phosphorylated on tyrosine 397
3pF	FAK phosphorylated on tyrosines in 400-900 range with active kinase activity
pP	active p38
pE	active ERK

The total amount of each protein is conserved and given a value of 1, so the inactive species fraction is calculated at each time point as 1 - Σ (active protein species).

Regulation of αSMA production

In the simplification of this system, we focused on p38 and ERK as the sole regulators of αSMA production. Phosphorylated p38 (pp38) promotes the production of αSMA, while pERK inhibits αSMA accumulation by slowing the rate of production. According to the model proposed

by Kawai-Kowase et al., ERK activated by FGF signaling prevents smooth muscle gene expression by interfering with serum response factor (SRF) function via an unknown mechanism.[5] We represented this in the model with the following equation:

$$\alpha SMA\ production = \frac{d[\alpha SMA]}{dt} = \frac{kaSMAf * [pp38]}{(kaSMAi * [pERK] + 1)} \quad . \qquad \text{Equation 1}$$

After initial experimental results showed a dramatically lower amount of αSMA in SYF-/- cells despite comparable levels of p38 phosphorylation, a modified equation for αSMA production was devised:

$$\alpha SMA\ production = \frac{d[\alpha SMA]}{dt} = \frac{kaSMAf * [pp38] * (0.01 + pS)}{(kaSMAi * [pERK] + 1)} \quad . \qquad \text{Equation 2}$$

Parameter estimation

Parameters were estimated by comparison with previously published models and by calculating the maximum relative activation changes in relevant experimental contexts. Both p38 and ERK are activated via cascades of signaling events downstream of growth factor receptors, Src, and FAK,[26,29] but these cascades are approximated as a single step with a lumped parameter for the sake of model simplicity. To estimate values for these lumped parameters, we measured αSMA expression and relative ERK and p38 phosphorylation in MEFs after 24 hours of treatment with 1 or 10 ng/ml TGF-β1 and FGF. We also tuned our model's sensitivity to changes in mechanical stiffness by measuring αSMA in cells plated on PDMS of stiffnesses ranging from 230 kPa to 2.14 MPa and on TCP (stiffness ~ 3 GPa).[48] The MATLAB optimization function *lsqnonlin* was used to vary up to three parameters at once to find the set of parameters which minimized the mean squared error (MSE) of the model fit to the growth factor sensitivity curves or the stiffness curve. While comparing candidate models, two parameters (kTpP and kαSMAf) were optimized to fit the growth factor calibration data set for each model.

Table 3: List of parameter values

Parameter	Description	Value [hr^{-1}]	Source
k1f	rate of β1 integrin adhesion and activation	23	estimated from [26]
k1r	rate of β1 integrin deactivation	0.567	estimated from [26]
k2f	rate of β3 integrin adhesion and activation	23	estimated from [26]
k2f	rate of β3 integrin deactivation	0.567	estimated from [26]
k3f	rate of TGF-β1 ligand attachment to TBR2 receptor	60	[28]
k3r	rate of TGF-β1 disassociation	15	estimated from [28]
kIpF	rate of β1 integrin activation of FAK	0.454	estimated from [7,26]
kIpS	rate of β3 integrin activation of Src	20.15	estimated from [11,26]
kTpS	rate of TGFβ receptor activation of Src	120	estimated from [20-21,37]
kSpF	rate of Src association with FAK and activation of secondary phosphorylation sites	29	estimated from [26-27,38]
KmSF	Michaelis-Menten constant for Src activation of FAK	0.1	estimated from [27]
kFAKpE	rate of FAK activation of ERK	240	estimated from [18,26]
kFGFpERK*	rate of FGF activation of ERK	40	estimated from [5,24]
kSpT	rate of Src phosphorylation of TBR2	40	estimated from [20,37]
KmST	Michaelis-Menten constant for Src activation of TBR2	0.1	estimated from [20,37]
kTpP*	rate of TGF-β1 activation of pp38	130.4-1076	estimated from [20,37]
kIpP*	rate of β1 integrin activation of p38	50	estimated from [8,39]
kPr	rate of p38 dephosphorylation	579.6	[30]
kEr	rate of ERK dephosphorylation	210	estimated from [26]
kSr	rate of Src dephosphorylation	432	estimated from [26]
kFr	rate of FAK dephosphorylation	48.35	estimated from [26]
kTr	rate of ligand-induced TBR2 deactivation	15	[28]
kE	intrinsic rate of ERK activation	10	estimated and optimized
kP	intrinsic rate of p38 activation	10	estimated and optimized
kαSMAf*	rate of p38 promotion of αSMA	1.1-11	estimated and optimized for each model
kαSMAi*	rate of ERK inhibition of αSMA production	20	estimated and optimized
kαSMAr	rate of αSMA degredation	1.03	estimated from [49]

Initial estimates of values were calculated from literature and varied to find the optimal parameter set. Parameters that were optimized to calibration data set indicated by *

Sensitivity analysis

Both the initial conditions and rate constants were varied over two decades around the primary estimation, and the relative change in output (αSMA concentration) and sensitivity coefficients *S* (relative change in output per relative change in parameter (*P*)) were calculated and ordered. This analysis provides insight into the bottlenecks and critical junctions where the system is more or less sensitive to perturbations

$$Sensitivity\ Parameter\ S = \frac{\Delta\ \alpha SMA/\alpha SMA_0}{\Delta\ P/P_0} \quad . \qquad \text{Equation 3}$$

Candidate model development and statistical comparison

We developed a set of candidate models which contain modified signaling mechanisms, reflecting different hypotheses. We used data set independent from the calibration curves used to refine the model to evaluate model fit and assess the likelihood of certain mechanisms. After simulating the set of 8 experiments with each candidate model, we calculated the χ^2 statistic for the set of experimental results. The χ^2 statistic is a metric for measuring model fit while accounting for variability in experimental data. When χ^2 is minimized, the agreement between the model prediction and the data is optimized

$$\chi^2 = \sum_{i=1}^{N} \frac{(y\_exp_i - y\_model_i)}{\sigma_i} \quad . \qquad \text{Equation 4}$$

Model evaluation using the using the Akaike information criterion (AIC)

The Akaike information criterion (AIC) is a metric for comparing models with different numbers of independent parameters (K), to attempt to optimize both the accuracy and the model simplicity, or parsimony, of different models variants[32,50]

$$AIC = 2K + 2((N/2) * \log(2\pi * MSE + 1)) \quad . \qquad \text{Equation 5}$$

N reflects the number of experimental data points and MSE is the mean squared error. This criterion can be used to great effect in determining the relative likelihood of multiple models.

Results

Src and FAK significantly regulate αSMA production via integrin signaling

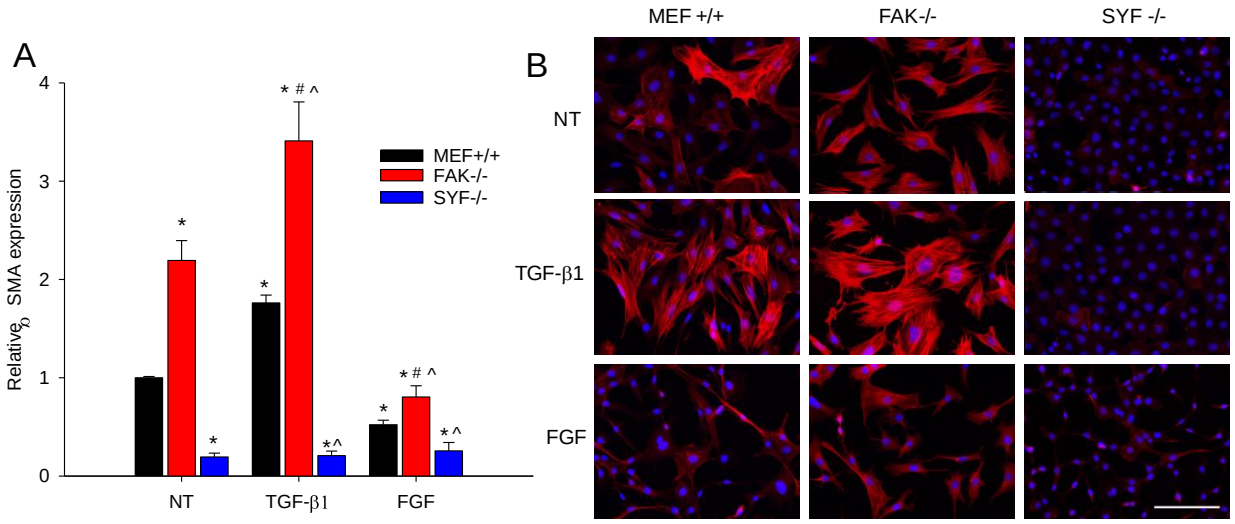

Figure 6: Focal adhesion proteins FAK and Src regulate myofibroblast differentiation. A. αSMA measured by ELISA after 24 hours of culture in serum free media, 1 ng/ml TGF-β1, or 10 ng/ml FGF. All FAK-/- and SYF-/- were all significantly different from the wild type MEF+/+ cells ($p < 0.001$). * denotes a significant difference between the NT and treated MEFs ($p < 0.05$). # denotes significant difference from the FAK-/- NT group. ^ denotes significant difference from the MEF+/+ sample under a given treatment. B. Representative images of αSMA stress fiber assembly in cells grown on fibronectin coated coverslips and stained for αSMA (red) and dapi nuclear stain (blue). The scale bar represents 50 μM.

MEFs with genetically deleted focal adhesion proteins express significantly different levels of αSMA in serum-free conditions than wild type cells (Figure 6). A two-way ANOVA shows significant interaction ($p < 0.001$) between cell type and treatment. SYF-/- cells expressed significantly less αSMA than MEF+/+ cells in all treatment groups (Figure 6A) and have noticeably altered morphology, with a rounded cell shape and few well-defined actin bundles or stress fibers (Figure 6B). Furthermore, there is no significant difference between

treatment groups within the SYF-/-. FAK-/- cells express significantly more αSMA than MEF+/+ cells regardless of treatment, and both growth factors cause a significant effect relative to untreated FAK-/- cells (Figure 6A). MEF+/+ and FAK-/- both have a fibroblast-like morphology, but in both treated and non-treated groups, a higher percentage of FAK-/- cells express αSMA (Figure 6B). TGF-β1 causes an increase in intensity and frequency of αSMA expression and stress fiber formation in both cell types (Figure 6B). FGF has the opposite effect, causing a loss of stress fibers and αSMA expression (Figure 6B). The inverted roles that FAK and Src play in regulating myofibroblast differentiation prompted a more detailed look at downstream signals.

TGF-β1, FGF, and stiffness modulate αSMA in a predictable manner

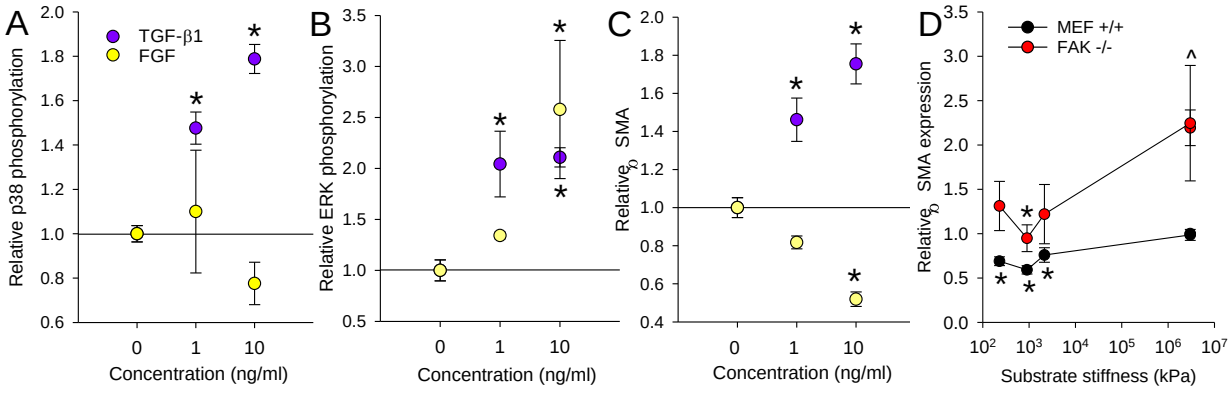

Figure 7: Calibration curves for reaction to growth factors and stiffness. A-C. Concentration-dependent changes to p38 and ERK activation and αSMA expression in response to TGF-β1 and FGF. D. Sensitivity to stiffness in production of αSMA in MEF+/+ and FAK-/- cells. * indicates significant difference from the no treatment/TCP condition within each cell type. ^ indicates significant difference from MEF+/+ sample within substrate. Active p38 and pERK data from densitometry of western blots (A-B) and αSMA determined from indirect ELISA (C-D). Average results are presented (n=4-12). These data were used to refine model parameters.

We conducted calibration experiments to correlate growth factor concentration and stiffness to internal signaling and regulation of αSMA and refine our initial estimates of lump

parameters. Our first calibration experiment (Figure 7A-C) clarified the relationship between growth factor concentration, equilibrium p38 and ERK phosphorylation, and αSMA expression in MEF+/+ cells. At 24 hours, there is no significant change in pp38 with treatment with 1 or 10 ng/mL FGF, but there is a significant log-linear increase proportional to TGF-β1 concentration (Figure 7A). There is significant ERK phosphorylation after 24 hours treatment with TGF-β1 that is independent of TGF-β1 concentration. There is also a significant increase in ERK activation with FGF treatment, which is highly dependent on FGF concentration (Figure 7B). These data were used to refine estimates of kTpP, kFGFpE, and kαSMAf (Table 3). The variability of the experimental measurements was considered in the optimization protocol; we selected the set of parameters which gave the minimum χ^2 statistic for each candidate model. By this technique, we achieved good agreement with our calibration curves, with χ^2 values as low as 8.12 ($p = 0.7$) for the set of 15 growth factor measurements, indicating that the model is a good fit to the data.

We next measured αSMA production over a range of substrate stiffness (Figure 7D) and found a statistically significant interaction between cell type and substrate stiffness ($p = 0.009$). αSMA production was significantly reduced when cells were cultured on PDMS, with the lowest αSMA expression corresponding to a PDMS stiffness of 900 kPa. There was no significant difference between αSMA expression on fibronectin-coated TCP and uncoated TCP in either cell type. αSMA in FAK-/- cells is significantly higher than in MEF+/+ ($p < 0.001$) on TCP (stiffness = 3E6 kPa) but is not statistically different at lower stiffness, indicating that FAK-/- are more sensitive to changes in stiffness than MEF+/+ cells. These data were also used to refine model fit and parameter estimation, especially in determining kIpP. χ^2 values as low as 2.9 ($p = 0.96$) were calculated for the set of 11 substrate measurements. After quantifying MAPK phosphorylation and aSMA expression at 24 hours, we directed our focus to the details of dynamic signaling.

TGF-β1 and FGF induce MAPK phosphorylation with different dynamic profiles

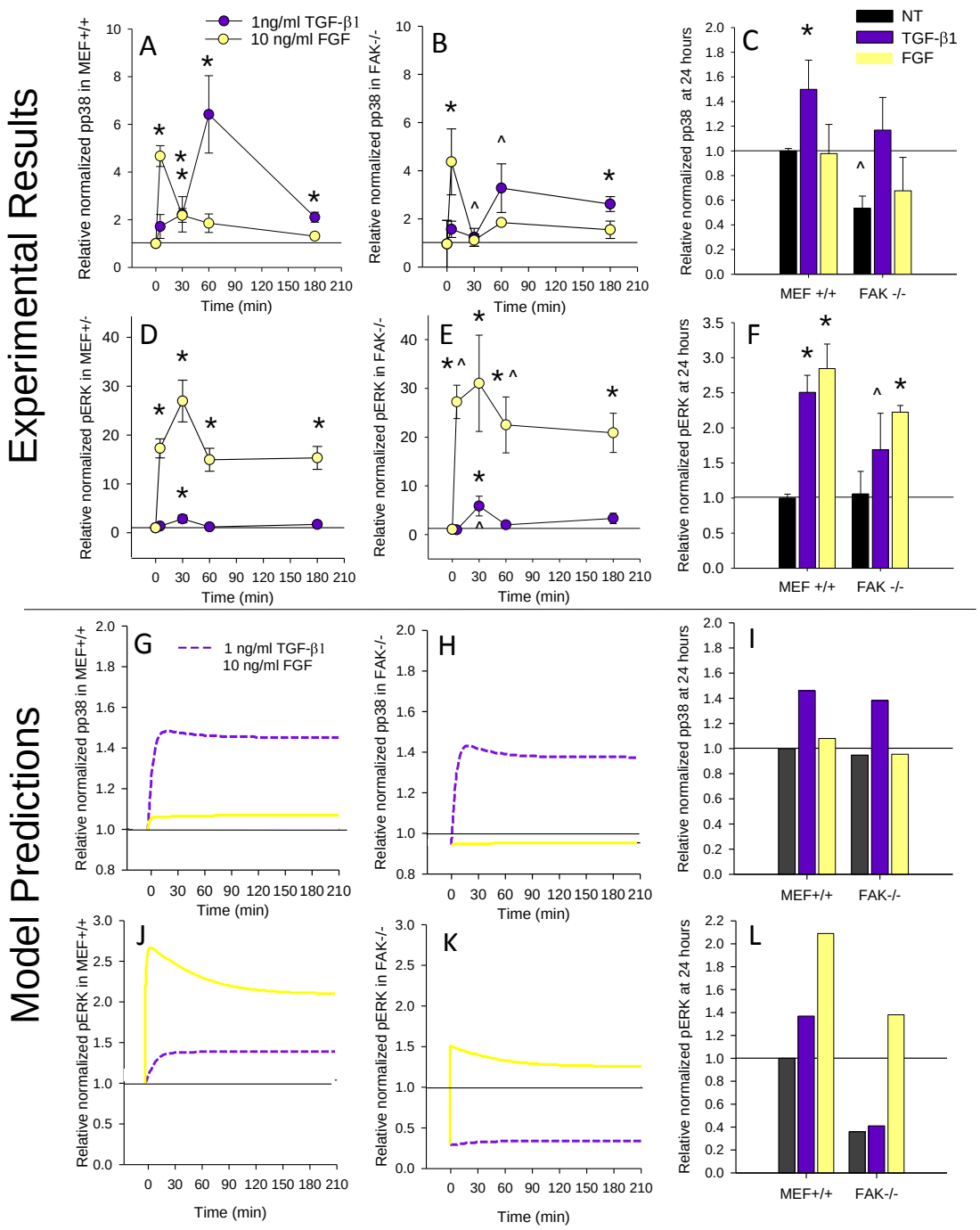

Figure 8: Different dynamic activation profiles for activation of ERK and p38. Averaged results of western blot densitometry analysis for pp38 (A-C) and ERK (D-F) activation over a 3 hour time course in MEF+/+ (A,D) and FAK -/- (B,E) cells treated with 1ng/ml TGF-β1 or 10 ng/ml FGF. Average p38 and ERK activity after 24 hours of treatment (C,F). * indicates significant difference ($p < 0.05$) from average no treatment within cell type and time course. ^ indicates significant difference ($p < 0.05$) from the MEF+/+ sample within treatment and time point. G-L are the model output values for the same quantities at the same time points.

Western blot data show significant and sustained p38 phosphorylation in response to TGF-β1, which peaks at 1 hour in both MEF+/+ and FAK-/- cells and remains significantly enhanced ($p = 0.017$) after 24 hours of treatment (Figure 8A-C). While the shape of this activation is consistent between cell types, the peak magnitude in the FAK-/- is significantly lower ($p = 0.007$). Steady state p38 phosphorylation at 24 hours is also significantly lower in FAK-/- cells relative to MEF+/+ ($p = 0.046$). In the same set of experiments, FGF induces a rapid increase in p38 phosphorylation, which attenuates to less than 1.5 fold of the non-treated group within one hour. FGF induced a dramatic increase in ERK phosphorylation in both cell types in five minutes that persisted for at least 3 hours (Figure 8D-E) and was still significantly elevated at 24 hours (Figure 8F). TGF-β1 induced a slight significant increase at 30 minutes, which faded to insignificance within 1 hour. However, both cell types show significantly enhanced ERK phosphorylation at 24 hours after treatment with TGF-β1 (Figure 8F). The dynamic ERK and p38 trends produced by model simulations share the same general shape as the experimental results, but the relative values are lower (Figure 8G-L). In this model, FGF does not directly activate p38, since the short duration and relatively low level of activation would not have a significant enough effect on αSMA content to justify the addition of model complexity. The model does predict a slight rise in p38 activation in MEFs following FGF stimulation that is transduced through FAK enhanced Src activation (Figure 8G).

Sensitivity analysis

Sensitivity analysis of the model with optimized parameters predicted that FAK-/- cells would be more sensitive to TGF-β1, FGF, and stiffness relative to MEF+/+ cells. Sensitivity analysis indicates that the model's response to TGF-β1 stimulation is most sensitive to changes in rate constants controlling the activation and deactivation of p38, Src, and TβR2 (Table 4). Of the boundary constraints and initial conditions, the total amount of β1 integrin has the largest effect on relative αSMA in MEF+/+ and FAK-/- models. While the rank and sign of sensitivities is conserved between MEF+/+ and FAK-/- models, the magnitude of the parameters is often higher in FAK-/- models. One interesting exception is kTpP, which is slightly lower in FAK-/- models (0.15 vs. 0.18). In MEF+/+ simulations, the response to FGF is most sensitive to the rate of FGF activation of ERK, the deactivation rate of FAK, and the rate of FAK-based activation by integrins. SYF-/- models have no reaction to TGF-β1, and their reaction to FGF is less sensitive to stiffness, FGF, and the rate of ERK activation by FGF than the MEF+/+ model. Sensitivity to both TGF-β1 and FGF and all the rate constants was predicted to increase on fibronectin-coated PDMS (stiffness 900 kPa) relative to TCP.

Table 4: Sensitivity analysis

	parameter	MEF+/+	FAK-/-	SYF-/-	MEF+/+ (on PDMS)
Inputs and boundary conditions	TGF-β1	0.19	0.23	0	0.28
	FGF*	-0.293	-0.32	-0.27	-0.33
	stiffness	-0.02	-0.03	0	-0.07
	β1-total	-0.30	-0.29	0	-0.39
	β3-total	-0.13	-0.22	0	-0.22
Rate constants	kTpP	0.18	0.15	0	0.24
	kIpP	-0.24	-0.26	0	-0.30
	kFGFpE*	-0.27	-0.31	-0.26	-0.29
	kaSMAf	-0.03	-0.09	0	-0.06
	kaSMAr	0.03	0.09	-0.18	0.06
	kaSMAi*	-0.09	-0.20	-0.17	-0.13

Subset of sensitivity coefficients (*S*) for each simulated cell type. Sensitivity analyzed after treatment with TGF-β1 or FGF (indicated by *). Results are shown for model 04, which contains direct dependence on Src

Model can predict results across substrate and cell type

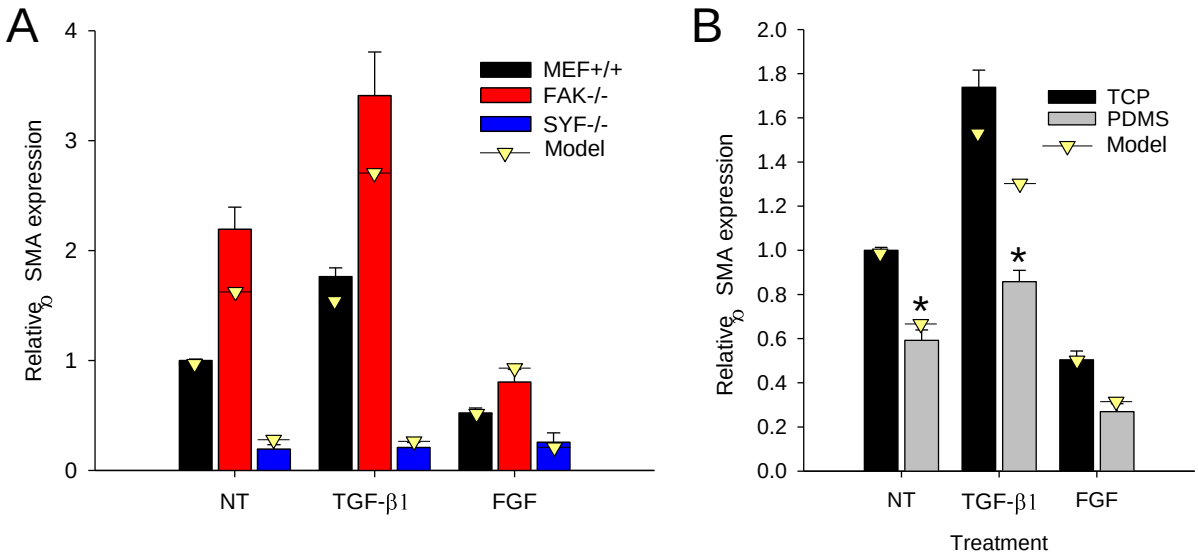

Figure 9: Model fit to TGF-β1 and FGF treatment across cell types and substrates. Average values of αSMA in MEF+/+ and FAK-/- cells (A) after 24 hour treatments and (B) in MEFs on TCP or fibronectin coated PDMS. Model predictions from model 04 with optimized parameters are plotted as triangles.

With optimized model parameters, we tested our model's ability to predict the effect of growth factor treatment on cells lacking Src and FAK that we observed *in vitro*. Figure 9A shows the model results plotted over the experimental results (same as Figure 6). We also measured the combined effects of treatment and substrate stiffness by treating cells plated on fibronectin-coated PDMS (Figure 9B) and found a statistically significant interaction between substrate and treatment ($p = 0.004$). Further, there is a significant difference ($p < 0.05$) between TCP and PDMS for non-treated and TGF-β1-treated cells, but not for FGF-treated cells. Within each substrate, both FGF and TGF-β1 treatment cause a significant ($p < 0.05$) change in αSMA expression. The model predictions are plotted over the experimental results, and were within a standard deviation for all but the TGF-β1-treated sample on PDMS.

Model comparisons

Eight candidate models were developed and evaluated to find the ideal fit to both steady state protein activation and dynamic protein phosphorylation events. The relative AIC (calculated as the difference between a given model's AIC and the minimum AIC) provides a useful criterion for eliminating inferior models and improving model parsimony. After parameter optimization of kαSMAf and kTpP for each model, simulated αSMA outputs were compared against the validation data set (Figure 9) and the MSE, χ^2 statistic, AIC, and ΔAIC were calculated (Table 5). The relative strength of evidence for any model (in comparison) can be estimated as $e^{-\Delta AIC/2}$. In other words, a model with ΔAIC greater than 10 is more than 148 times less likely than the best model.[32,50] We found that the model with the lowest AIC also had a very low MSE and χ^2 while maintaining close agreement with the dynamic pp38 and pERK curves observed experimentally. Model 03 contained the modified αSMA production equation (Equation 2) which has a Src-dependent term and negative feedback to Src but did not contain negative feedback to ERK. ΔAIC for the equivalent model (02) with the unmodified equation for αSMA production (Equation 1) was 5.91, giving strong evidence that the Src-dependent term is supported by the data. Model 15 did not have a negative feedback loop for ERK, which means that the observed change in relative ERK phosphorylation from 3 hours to 24 hours (Figure 8D-F) could not be replicated by this model. The equivalent model with negative feedback to ERK (model 04) had an ΔAIC of 1, so it is reasonably close to the optimal model. Furthermore, after optimization model 04 was able to achieve lower χ^2 values and better matching to the calibration data. Model 04 simulations are presented in Figures 4 and 5. Model 07 had the lowest MSE and best fit to the experimental data set via the addition of a calpain feedback loop which degrades β3 integrin and FAK, but this addition of model complexity increased the AIC score above the simpler models 03 and 04. These data indicate that the features of the model presented above have reasonable support from the data.

Table 5: Model comparison and statistical analysis

Model	Features	MSE	χ^2	ΔAIC
01	No Src dependency or Src feedback or ERK feedback	0.768	541.96	6.66
02	No Src dependency term, but Src and ERK feedback	0.499	278.9	6.03
04*	Src dependency, Src and ERK feedback	0.090	24.79	0.93
05	Model 04 without stiffness dependence of IpP	0.163	51.23	1.96
06*	Model 04 with β3 integrin positive feedback	0.083	19.14	2.82
07*	Model 03 with Calpain negative feedback to ERK	0.019	16.46	3.85
08	More direct αSMA dependence on ERK	0.052	44.47	0.35
03*	Src dependency and Src feedback	0.029	18.64	0

* Indicates that the χ^2 value for the given model has a $p < 0.05$ for a χ^2 distribution with 15 degrees of freedom, indicating that the model predictions are not significantly different from the experimental data set.

Discussion

The role of Src

Using genetically modified MEFs, we have highlighted the importance of Src family kinases and FAK in the regulation of myofibroblast differentiation. Our results demonstrate a profound inhibitory effect of removing Src on αSMA production and stress fiber assembly. Densitometry revealed comparable levels of p38 and ERK phosphorylation in SYF-/- cells relative to MEF+/+ cells (data not shown), so the effect is likely operating through a different mechanism. This prompted the addition of a Src-dependent term to the αSMA production equation to capture the significant αSMA reduction in SYF-/- cells (Equation 2). Without the addition of that term, SYF-/- cells *in silico* behave similarly to FAK-/-, since the absence of Src prevents the activation of FAK kinase ability. It is likely that signaling downstream of Cas and other Src substrates is necessary for proper αSMA synthesis. TGF-β1 signals to TGF-β activated kinase 1 and subsequent αSMA production is significantly reduced with Src inhibition and the removal of FAK.[51] This result is consistent with recent reports of Src's prominent role in non-canonical TGF-β1 signaling in the context of myofibroblast differentiation.[21]

The role of FAK

Interestingly, the absence of FAK, a protein which is known to enhance Src activation and signal to p38, caused a significant increase in αSMA. Given its complex role in multiple signaling cascades, it is not surprising that reports of the effect of FAK on myofibroblast differentiation vary. Blocking FAK expression in cardiac fibroblasts with siRNA has been shown to decrease force-induced αSMA promoter activity.[41] Furthermore, Ding et al. (2008) have reported that αSMA production in serum-free conditions and after TGF-β1 treatment is higher in FAK expressing MEFs compared with FAK-/- counterparts. They found that FAK-related non-kinase blocked TGF-β1-induced FAK activation, p38 and pERK phosphorylation, and αSMA upregulation in primary fibroblasts and in FAK-/- cells.[52] Alternatively, others have reported that FAK is involved in FGF signaling to ERK in response to FGF cells, and FAK-/- cells contain enhanced αSMA accumulation and persistence after treatment with FGF.[5,24] They also report reduced basal ERK phosphorylation in FAK-/- cells, and proposed a model for FGF signaling to ERK requiring FAK.[24] This informed the development of our model and is consistent with the decreased initial ERK phosphorylation and increased αSMA that our model predicted. Additionally, we found that FGF was able to induce significant ERK phosphorylation and lower αSMA in the absence of FAK, which indicates that FAK is not required for FGF- and ERK-based inhibition of αSMA.

Integrin mechanotransduction

One of the major goals of this project was to clarify the interactions between growth factor and integrin signaling in the regulation of myofibroblast differentiation. We first showed that decreasing substrate stiffness can significantly lower the expression of αSMA in MEFs through a fibronectin-integrin interaction that is significantly altered in FAK-/- cells (Figure 7D). Sensitivity analysis of the model predicted that FAK-/- cells would be more sensitive to changes

in stiffness, which is observed in the experimental data (Figure 7D). The relationship between αSMA and stiffness has been shown previously and is correlated with changes in p38 activation.[8] Both β1 and β3 integrins have been shown to have mechanosensitive capabilities and are involved in outside-in signaling to intracellular kinases like FAK and Src.[6-7] Our model uses an activation function proportional to the log of stiffness to simulate integrin activation of FAK, Src, and p38, which gives good agreement with experimental results (Figure 7D). We further showed the combinatorial effect of substrate changes and growth factor treatments and found a significant interaction, justifying the development of an integrated signaling model (Figure 9B). All the data in Figure 9 were well matched by a model whose parameters had been optimized to an independent data set (Figure 7), which strengthens our proposed model on the roles on p38 and pERK. The largest discrepancy between model prediction and experimental results, response to TGF-β1 in cells on PDMS, highlights an area needing more detailed investigation: the effect of stiffness and integrin signaling on TGF-β1 pathways. β3 integrins are known to interact with TGF-β1 signaling to Src and p38[53] and are a likely target for further insights.

Time course results

Surprisingly, our time course results show that ERK phosphorylation in non-treated FAK-/- cells is not significantly different from MEF+/+ at 24 hours and is significantly higher at 30 minutes. Sensitivity analysis of the model predicted that FAK-/- cells would be more sensitive to changes in TGF-β1 and FGF. Our experimental results seem to confirm that FAK-/- cells have a higher sensitivity to environmental pertubations when the media is changed at the start of the time course. ERK's specific role in αSMA regulation has also presented in multiple perspectives. Some have argued that ERK is necessary for TGF-β1 induced activation,[52,54] while others proposed a largely inhibitory role.[5,24,55-56] Several groups have shown that MEK1/2 inhibition significantly increases αSMA expression in fibroblast-like cells.[57-58] ERK is a major player in a

large set of signaling pathways, which interacts with several other MAPKs to transduce a variety of signals. For instance, ERK is necessary for TGF-β1-induced upregulation of collagen-1 and cadherin 11, two other markers of myofibroblast differentiation.[57,59] One of the goals of this project was to investigate the possibility of matching the observed upregulation of ERK by TGF-β1 and FGF in a model with a relatively straightforward αSMA regulatory scheme.

Novel findings from model analysis

We developed a computational model of these overlapping signaling pathways and a set of tools for network analysis and hypothesis generation. Sensitivity analysis of the model predicted higher sensitivity to FGF and stiffness in FAK-/- cells relative to MEF+/+. Experimentally, FAK-/- cells demonstrated a larger relative change in response to FGF than in wild type cells (63% or 49% decrease, respectively), but a smaller relative response to TGF-β1 (55% or 73% increase, respectively) (Figure 9A). According to the constitutive equation for αSMA activation, the sensitivity of equilibrium αSMA to both p38 and pERK is inversely proportional to ERK activation, so lower basal ERK activation, as found in FAK-/- cells, should cause higher sensitivity to all parameters which affect ERK and p38 activation. Functionally, equations 1 and 2 mean that the presence of active ERK dampens the sensitivity of the system to changes in MAPK activation. Since the growth factors present in serum can cause a significant increase in ERK activation, we performed all of our ELISA and western blot experiments in serum-free conditions. Sensitivity to both TGF-β1 and FGF was predicted to increase with decreasing stiffness, and was observed in the case of FGF (54.5% vs. 49.5% decrease) though the reverse is true for TGF-β1 (45% vs. 73% increase) (Figure 9B). Further investigation into altered signaling on softer substrates could help clarify this discrepancy. Our model comparison revealed that a direct dependency on active Src greatly enhanced the quality of model fit. It also indicated that including more complex network interactions, like calpain-based negative feedback, can improve model accuracy, but not enough to justify additional

model complexity. Future analysis of the model using larger calibration and validation data sets will give more insight into the dynamics of myofibroblast regulation. Overall, this study demonstrates the feasibility of p38/ERK/Src-based regulation of αSMA production during fibroblast differentiation.

Conclusions

In this study we have demonstrated that an ODE-based computational model of relative protein expression can successfully capture a subset of the dynamic and steady-state events observed during fibroblast differentiation. We have further shown that the mechanism of Src/p38/ERK-based regulation of αSMA as described herein is a feasible model for regulation of myofibroblast differentiation. Model simulations were able to replicate the dual, dynamic profile of TGF-β1 and FGF signaling to p38 and pERK and show that despite the fact that it increases with TGF-β1 treatment, ERK may be acting primarily as a negative regulator of αSMA. Our results indicate that Src is crucial for αSMA synthesis and demonstrate that FAK plays an important role in integrating signals for the regulation of αSMA production and myofibroblast differentiation.

CHAPTER III

CONCLUSIONS AND FUTURE WORK

Conclusions

The result from this work is a flexible model describing how Src, FAK, ERK and p38 integrate signals from integrins, TGF-β1, and FGF to regulate myofibroblast differentiation. We have demonstrated that Src is necessary for TGF-β1 and integrin-induced myofibroblast activation, while FAK plays an inhibitory role. We have further shown that TGF-β1 and FGF stimulate p38 and ERK phosphorylation with different dynamic profiles. Finally, we have demonstrated that a relatively simple model of αSMA regulation with positive dependency on Src and p38 and negative dependency on ERK is a feasible explanation of observed trends in myofibroblast differentiation.

Future Work

Future experiments to probe the dynamics of this system will provide greater insights into this cellular process and strengthen the claims of our model. An ongoing study with β3 integrins will provide more experimental support for the initial activation steps of integrin clustering and Src activation. Transfection of MEFs with fluorescently labeled β3 integrins allows for visualization of integrin clustering on fibronectin-coated surfaces in control conditions and after treatment with TGF-β1. Co-staining for active Src and western blots will reveal the dynamics of Src activation and any interaction between TGF-β1 and β3 integrins. Preliminary results indicate that TGF-β1 treatment alone is sufficient to induce inside-out β3 integrin clustering and colocalization with activated Src. This interaction could have serious implications in the progression of myofibroblast activation. This study can also be useful in estimating the relevant local forces experienced by the integrins. Fluorescent images of integrin cluster

locations and aSMA stress fiber distribution will be used to build cell-specific finite element mechanical models which can be used to estimate local and average forces applied to integrins under different conditions.

Future work will also expand the focus to examine other markers of myofibroblast differentiation, such as cadherin 11 and collagen 1. Preliminary results show that both cadherin 11 and collagen 1 are significantly reduced in both FAK-/- and SYF-/- cells relative to MEF+/+. These data indicate that the traditional markers of myofibroblasts have divergent regulation via FAK. Immunostaining of MEF+/+ confirms that cadherin 11 and aSMA are not always coexpressed. ERK is required for TGF-β1-induced upregulation of both cadherin 11 and collagen, so it is likely that disrupted signaling through ERK in the FAK-/- cells is responsible for the observed differences in myofibroblast marker expression. This hypothesis will be more thoroughly investigated through use of U0126, a MEK ½ inhibitor that will block ERK phosphorylation.

Finally, this work will be targeted at a tissue-specific fibroblast population that has immense clinical relevance. Cardiac fibroblasts are responsible for formation and maintenance of the connective tissue structure of the heart. Serious remodeling defects like cardiac hypertrophy and scar formation after myocardial infarction contribute significantly to heart failure and are linked to cardiac fibroblast function. The new insights into the signaling that regulates myofibroblast differentiation gained in this study will inform our study of cardiac fibroblasts *in vitro* and *in vivo.*

APPENDIX A

Model considerations

This ODE model was developed and analyzed in MATLAB. The initial conditions of all active protein species were set at 0.001, the environmental conditions were matched to experimental levels, and the model was allowed to equilibrate by simulation of 24 hours of culture. Using the steady state variable values as a starting point, the dynamic response of the system to treatments like addition of TGF-β1 or FGF was simulated. Details on some of the specific activation steps can be found below.

Integrin activation and clustering

Both intracellular and extracellular cues can lead to and strengthen integrin activation, but this model focuses on "outside-in" signaling linked to adhesion to ECM proteins collagen and fibronectin. Integrins with a β1 subunit can adhere to both fibronectin and collagen and are known to stimulate the activation of the autophosphorylation site on FAK (y397).[7,26,60] Integrins containing the β3 subunit are activated by adhesion to the RGD subunit of fibronectin and can directly activate Src.[11-12] In both cases, integrin clustering reinforces integrin activation and allows greater signaling to downstream targets like Src and FAK. In the model, dynamic clustering is approximated by a simple dimerization step whereby ECM adhesion leads to a pair of activated β1 or β3 integrins which in turn stimulate FAK or Src activation at a proportional rate. This activation is also modulated by the log of the substrate stiffness, since β1 integrin subunits are known to activate the autophosphorylation site tyrosine 397 of FAK proportionally to the log of substrate stiffness.[7] P38 phosphorylation is sensitive to stiffness, and since β1 integrin is known to activate p38, all candidate models besides model 5 contain a stiffness-dependent activation of p38.[8,61]

Equation for β1 integrin activation and clustering:

$$B1onrate = k1f * FN * B1off^2 + k1f * Cl * B1off^2 - k1r * B1on$$

Equation for β1 integrin activation of FAK:

$$IpFrate = kIpF * log10(10 * stiffness) * B1on * F$$

Since MEFs are known to excrete fibrillar collagen and fibronectin in culture,[60,62] especially on stiff substrates, we assumed that cells plated on plastic had the equivalent of 20 percent of fibronectin present on a fibronectin-coated surface (assumed to be a maximum value of 1) and 10 percent of collagen that would be present on a collagen-coated surface (assumed to be a maximum value of 1).

Src-FAK interactions

Src and FAK have a complex series of interactions and cross-phosphorylation which require special attention in the model. FAK is a large scaffolding protein with several phosphorylation sites and interactions with a large number of other proteins. β1 integrin activation leads to phosphorylation of the autophosphorylation site of FAK, tyrosine 397 [60]. An association of the SH2 domain of the Src protein with the phosphorylated tyrosine 397 promotes the open conformation of Src that prevents deactivation by phosphorylation of tyrosine 527 and allows for more phosphorylation of tyrosine 416, increasing in Src kinase activity.[17,63] When Src associates with FAK in this manner it can also cause the phosphorylation of FAK at tyrosines 576, 577, 861, 925, and others. This secondary phosphorylation activates the kinase activity of FAK and allows for signaling to downstream targets like ERK and p38. It also promotes FAK autophosphorylation of y397 of surrounding FAK proteins.[38] This complex relationship is represented in the model by a three-step activation scheme for FAK: inactive (FAK), phosphorylated on 397 (pFAK), and in a complex with Src with the additional tyrosine residues of FAK phosphorylated (3pF). Src also has three active states: inactive (Src), active (pSrc), and

in the Src/FAK complex. A similar Src/FAK activation model was used in a model developed by Caron-Lormier et al. in 2004.[27] Whether or not Src in complex with FAK is able to phosphorylate pp38 or perform other roles is one of the questions investigated by model comparisons.

Equation for Src activation of pF to form 3pF Src/FAK complex:

$$SpFrate = kSpF * S * pF + 10 * kSpF * pS * pF/(KmSF + pF)$$

Ten percent of the complex returns to pS phase after dissolution of the 3pF state, and all of it returns to the pF state.

TGF-β1 signaling and Src based regulation

Src has an important role in non-canonical TGF-β1 signaling to p38 in the regulation of myofibroblast differentiation. After TGF-β1 ligand binding, the 284 tyrosine residue on TGF-β1-receptor 2 (TBR2) must be phosphorylated by Src for TGF-β1 induced activation of p38 to occur.[20] This two-step activation is accounted for by the inclusion of an intermediate activation state for the TBR2 receptor, which is associated with a TGF-β1 ligand and able to activate Src kinase activity but unable to activate p38. The phosphorylated form of the receptor (pTBR2) is able to induce p38 phosphorylation and Src activation.[20] Half of the TBR2 becomes recycled to a -ree state after dephosphorylation.

Equations governing TGF-β1 signaling:

$$TBRTrate = k3f * Tgfb * TBR2off - k3r * TBR2T$$
$$TpSrate = kTpS * S * (pTBR2 + TBR2T)$$
$$SpTrate = kSpT * TBR2T * pS/(KmST + TBR2T)$$
$$dTBR2T/dt = TBRTrate - SpTrate - 0.5 * dpT$$

Dynamic feedback loops

A major goal of this study was to understand the crosstalk between direct TGF-β1 and FGF signaling to p38 and ERK. To account for the transient nature of signaling to both p38 and ERK, some of the candidate models included negative feedback to Src and ERK. The Src feedback loop approximates the role of Csk to limit Src kinase activity as focal adhesions mature over time. Src and FAK activation signals through Cas and causes an accumulation of paxillin in focal adhesions roughly proportional to the accumulation of αSMA.[64] Paxillin recruits Csk, which lowers Src activity [12,65]. Another potentially relevant feedback mechanism is calpain, which is activated by ERK and degrades FAK and β3 integrin.[66] Finally, we simulated a positive feedback loop by which p38 stimulates β3 integrin expression.[67] These mechanisms add complexity to the model but also make the model more relevant to the biological system and provide closer matching with the dynamic phosphorylation events.

Equation for Src feedback loop:

$$dppS = -kSr * pS - kSr * 100 * aSMA * pS$$

Equation for ERK feedback loop:

$$dppE = -kEr * pERK - 10 * pERK/aSMA$$

Equations for calpain based feedback (incorporated in model 07):

$$calrate = kEaC * pERK - cal * 0.5$$

$$B3onrate = \cdots - kcaldeg * cal * B3on$$

$$dpF = \cdots - kcaldeg * cal * pF$$

Equations for p38- β3 integrin feedback (incorporated in model 06):

$$B3onrate = \cdots + kPB3 * pP * B3off^2$$

Example MATLAB code for candidate model 1

ode15s was used to solve

```
function dydt = IntegrinModelODEfunc01 (t,y,params)
% defines the system of ODEs describing the model
% written by Alison Schroer
% Vanderbilt University, 1/17/2012

% Assign names for parameter values and state variables

%% define parameters
k1f = params(1);
k1r = params(2);
k2f = params(3);
k2r = params(4);
kIpF = params(5);
kIpS = params(6);
kFpF = params(7);
kTpS = params(8);
kSpF = params(9);
kFakpE = params(10);
kFGFpERK = params(11);
kSpT = params(12);
kTpP = params(13);
kSpP = params(14);
kIpP = params(15);
KmFF = params(16);
KmST = params(17);
KmSF = params(18);
kPdE = params(19);
kP= params(20);
kE = params(21);
kStiff = params(22);
kSr = params(23);
kFr = params(24);
kPr = params(25);
KmPr = params(26);
kEr = params(27);
B1tot = params(28);
B3tot = params(29);
Ftot = params(30);
Stot = params(31);
Ptot = params(32);
ERKtot = params(33);
TBR2 = params(34);
Fn = params(35);
Cl = params(36);
Tgfb = params(37);
FGF = params(38);
stiffness = params(39);
kaSMAf = params(40);
kaSMAr = params(41);
kaSMAi = params(42);
kTr = params(43);
k3f = params(44);
```

```
k3r = params(45);

B1on = y (1);   %On state reflective of engagement with engagement with ECM
and clustering
B3on = y (2);   %On state reflective of engagement with engagement with ECM
and clustering
TBR2T = y (3);
pTBR2 = y (4);
pS = y (5);
pF = y (6);
p3F = y(7);
pP = y (8);
pERK = y(9);
aSMA = y (10);

% Conservation equations
B3off = B3tot-2*B3on;
B1off = B1tot-2*B1on;
F = Ftot-pF-p3F;
S = Stot-pS-p3F;
P = Ptot-pP;
ERK = ERKtot-pERK;
TBR2off = TBR2 - pTBR2 - TBR2T;

% Reaction rates
B1onrate = k1f*Fn*B1off^2 +k1f*Cl*B1off^2 - k1r*B1on;
B3onrate = k2f*Fn*B3off^2 - k2r*B3on;
TBRTrate = k3f*Tgfb*TBR2off - k3r*(TBR2T);
IpFrate = log10(10*stiffness)*kIpF*B1on*F;
IpSrate = log10(10*stiffness)*kIpS*B3on*S;
IpPrate = log10(stiffness)* kIpP*B1on*P;

TpSrate = kTpS*S*(TBR2T);
SpTrate = kSpT*TBR2T*pS/(KmST+TBR2T);
FpFrate = kFpF*F*p3F/(KmFF+F);
SpFrate = kSpF*S*pF+10*kSpF*pS*pF/(KmSF+pF);
SpPrate = kSpP*pS*P;
TpPrate = kTpP*pTBR2*P;

FpErate = kFakpE*p3F*ERK;
pERKrate = FGF*kFGFpERK*ERK;

aSMAproduction = kaSMAf*pP/(kaSMAi*pERK+1);%
aSMAdegredation =  - kaSMAr*aSMA;

dpT = - kTr*pTBR2;
dppP = - kPr*pP;
dppS = - kSr*pS;
dppF = - kFr*pF;
dppERK = -kEr*pERK;

% Differential equations;
dB1on = B1onrate;
dB3on = B3onrate;
dTBR2T = TBRTrate - SpTrate - 0.5*dpT;
```

```
dpTBR2 = SpTrate + dpT;
dpS = IpSrate+TpSrate+dppS+kFr*p3F/10;
dpF = IpFrate+FpFrate+dppF+kFr*p3F-SpFrate;
dp3F = SpFrate-kFr*p3F;
dpP = SpPrate+IpPrate+TpPrate+dppP+kP*P;
dpERK = FpErate+pERKrate+dppERK+kE*ERK;
daSMA = aSMAproduction+aSMAdegredation;

dydt = [dB1on;dB3on;dTBR2T;dpTBR2;dpS;dpF;dp3F;dpP;dpERK;daSMA;0];
% Reassemble differential equations
```

REFERENCES

1. Hinz, B. & Gabbiani, G. Cell-matrix and cell-cell contacts of myofibroblasts: role in connective tissue remodeling. *Thromb Haemostasis* **90**, 993-1002 (2003).

2. Tomasek, J.J., Gabbiani, G., Hinz, B., Chaponnier, C. & Brown, R.A. Myofibroblasts and mechano-regulation of connective tissue remodelling. *Nat Rev Mol Cell Biol* **3**, 349-363 (2002).

3. Merryman, W.D.*, et al.* Synergistic effects of cyclic tension and transforming growth factor-beta1 on the aortic valve myofibroblast. *Cardiovasc Pathol* **16**, 268-276 (2007).

4. Bottcher, R.T. & Niehrs, C. Fibroblast growth factor signaling during early vertebrate development. *Endocr Rev* **26**, 63-77 (2005).

5. Kawai-Kowase, K.*, et al.* Basic fibroblast growth factor antagonizes transforming growth factor-beta1-induced smooth muscle gene expression through extracellular signal-regulated kinase 1/2 signaling pathway activation. *Arterioscler Thromb Vasc Biol* **24**, 1384-1390 (2004).

6. Roca-Cusachs, P., Gauthier, N.C., Del Rio, A. & Sheetz, M.P. Clustering of alpha(5)beta(1) integrins determines adhesion strength whereas alpha(v)beta(3) and talin enable mechanotransduction. *Proc Natl Acad Sci U S A* **106**, 16245-16250 (2009).

7. Friedland, J.C., Lee, M.H. & Boettiger, D. Mechanically activated integrin switch controls alpha5beta1 function. *Science* **323**, 642-644 (2009).

8. Meyer-ter-Vehn, T., Han, H., Grehn, F. & Schlunck, G. Extracellular matrix elasticity modulates TGF-beta-induced p38 activation and myofibroblast transdifferentiation in human tenon fibroblasts. *Invest Ophthalmol Vis Sci* **52**, 9149-9155 (2011).

9. Legate, K.R., Wickstrom, S.A. & Fassler, R. Genetic and cell biological analysis of integrin outside-in signaling. *Genes Dev* **23**, 397-418 (2009).

10. Fornaro, M. & Languino, L.R. Alternatively spliced variants: a new view of the integrin cytoplasmic domain. *Matrix Biol* **16**, 185-193 (1997).

11. Arias-Salgado, E.G.*, et al.* Src kinase activation by direct interaction with the integrin beta cytoplasmic domain. *Proc Natl Acad Sci U S A* **100**, 13298-13302 (2003).

12. Obergfell, A.*, et al.* Coordinate interactions of Csk, Src, and Syk kinases with [alpha]IIb[beta]3 initiate integrin signaling to the cytoskeleton. *J Cell Biol* **157**, 265-275 (2002).

13. Michael, K.E., Dumbauld, D.W., Burns, K.L., Hanks, S.K. & Garcia, A.J. Focal adhesion kinase modulates cell adhesion strengthening via integrin activation. *Mol Biol Cell* **20**, 2508-2519 (2009).

14. Baker, E.L. & Zaman, M.H. The biomechanical integrin. *J Biomech* **43**, 38-44 (2010).

15. Katsumi, A., Orr, A.W., Tzima, E. & Schwartz, M.A. Integrins in mechanotransduction. *J Biol Chem* **279**, 12001-12004 (2004).

16. Mitra, S.K. & Schlaepfer, D.D. Integrin-regulated FAK-Src signaling in normal and cancer cells. *Curr Opin Cell Biol* **18**, 516-523 (2006).

17. Roskoski, R., Jr. Src kinase regulation by phosphorylation and dephosphorylation. *Biochem Biophys Res Commun* **331**, 1-14 (2005).

18. Wang, J.G., Miyazu, M., Matsushita, E., Sokabe, M. & Naruse, K. Uniaxial cyclic stretch induces focal adhesion kinase (FAK) tyrosine phosphorylation followed by mitogen-activated protein kinase (MAPK) activation. *Biochem Biophys Res Commun* **288**, 356-361 (2001).

19. Watanabe, T.*, et al.* Adaptor protein Crk induces Src-dependent activation of p38 MAPK in regulation of synovial sarcoma cell proliferation. *Mol Cancer Res* **7**, 1582-1592 (2009).

20. Galliher, A.J. & Schiemann, W.P. Src phosphorylates Tyr284 in TGF-beta type II receptor and regulates TGF-beta stimulation of p38 MAPK during breast cancer cell proliferation and invasion. *Cancer Res* **67**, 3752-3758 (2007).

21. Hutcheson, J.D., Ryzhova, L.M., Setola, V. & Merryman, W.D. 5-HT(2B) antagonism arrests non-canonical TGF-beta1-induced valvular myofibroblast differentiation. *J Mol Cell Cardiol* **53**, 707-714 (2012).

22. Hanafusa, H.*, et al.* Involvement of the p38 mitogen-activated protein kinase pathway in transforming growth factor-beta-induced gene expression. *J Biol Chem* **274**, 27161-27167 (1999).

23. Elberg, G.*, et al.* MKL1 mediates TGF-beta1-induced alpha-smooth muscle actin expression in human renal epithelial cells. *Am J Physiol Renal Physiol* **294**, F1116-1128 (2008).

24. Greenberg, R.S.*, et al.* FAK-dependent regulation of myofibroblast differentiation. *Faseb J* **20**, 1006-1008 (2006).

25. Maher, P. p38 mitogen-activated protein kinase activation is required for fibroblast growth factor-2-stimulated cell proliferation but not differentiation. *J Biol Chem* **274**, 17491-17498 (1999).

26. Yee, K.L., Weaver, V.M. & Hammer, D.A. Integrin-mediated signalling through the MAP-kinase pathway. *Iet Syst Biol* **2**, 8-15 (2008).

27. Caron-Lormier, G. & Berry, H. Amplification and oscillations in the FAK/Src kinase system during integrin signaling. *J Theor Biol* **232**, 235-248 (2005).

28. Vilar, J.M., Jansen, R. & Sander, C. Signal processing in the TGF-beta superfamily ligand-receptor network. *PLoS Comput Biol* **2**, e3 (2006).

29. Hendriks, B.S., Hua, F. & Chabot, J.R. Analysis of mechanistic pathway models in drug discovery: p38 pathway. *Biotechnol Prog* **24**, 96-109 (2008).

30. Khanna, P.*, et al.* Model Simulations Reveal VCAM-1 Augment PAK Activation Rates to Amplify p38 MAPK and VE-Cadherin Phosphorylation. *Cell Mol Bioeng* **4**, 656-669 (2011).

31. Janes, K.A.*, et al.* A systems model of signaling identifies a molecular basis set for cytokine-induced apoptosis. *Science* **310**, 1646-1653 (2005).

32. Shankaran, H.*, et al.* Integrated experimental and model-based analysis reveals the spatial aspects of EGFR activation dynamics. *Mol Biosyst* **8**, 2868-2882 (2012).

33. Wang, J., Chen, H., Seth, A. & McCulloch, C.A. Mechanical force regulation of myofibroblast differentiation in cardiac fibroblasts. *Am J Physiol Heart Circ Physiol* **285**, H1871-1881 (2003).

34. Junttila, M.R., Li, S.P. & Westermarck, J. Phosphatase-mediated crosstalk between MAPK signaling pathways in the regulation of cell survival. *FASEB J* **22**, 954-965 (2008).

35. Plopper, G.E., McNamee, H.P., Dike, L.E., Bojanowski, K. & Ingber, D.E. Convergence of integrin and growth factor receptor signaling pathways within the focal adhesion complex. *Mol Biol Cell* **6**, 1349-1365 (1995).

36. WD, S.-L.M.a.M. The role of Src in strain- and ligand-dependent phenotypic modulation of mouse embryonic fibroblasts. in *Proceedings in Bioengineering (ASME)* (Farmington, PA,, 2011).

37. Galliher, A.J. & Schiemann, W.P. Beta3 integrin and Src facilitate transforming growth factor-beta mediated induction of epithelial-mesenchymal transition in mammary epithelial cells. *Breast Cancer Res* **8**, R42 (2006).

38. Thomas, J.W.*, et al.* SH2- and SH3-mediated interactions between focal adhesion kinase and Src. *J Biol Chem* **273**, 577-583 (1998).

39. Ivaska, J.*, et al.* Integrin alpha2beta1 mediates isoform-specific activation of p38 and upregulation of collagen gene transcription by a mechanism involving the alpha2 cytoplasmic tail. *J Cell Biol* **147**, 401-416 (1999).

40. Eubanks, T.R., Greenberg, J.J., Dobrin, P.B., Harford, F.J. & Gamelli, R.L. The effects of different corticosteroids on the healing colon anastomosis and cecum in a rat model. *Am Surg* **63**, 266-269 (1997).

41. Chan, M.W., Arora, P.D., Bozavikov, P. & McCulloch, C.A. FAK, PIP5KIgamma and gelsolin cooperatively mediate force-induced expression of alpha-smooth muscle actin. *J Cell Sci* **122**, 2769-2781 (2009).

42. Faust, D.*, et al.* Differential p38-dependent signalling in response to cellular stress and mitogenic stimulation in fibroblasts. *Cell Commun Signal* **10**, 6 (2012).

43. Bajikar, S.S. & Janes, K.A. Multiscale models of cell signaling. *Ann Biomed Eng* **40**, 2319-2327 (2012).

44. Janes, K.A., Reinhardt, H.C. & Yaffe, M.B. Cytokine-induced signaling networks prioritize dynamic range over signal strength. *Cell* **135**, 343-354 (2008).

45. Ilic, D.*, et al.* Reduced cell motility and enhanced focal adhesion contact formation in cells from FAK-deficient mice. *Nature* **377**, 539-544 (1995).

46. Brown, X.Q., Ookawa, K. & Wong, J.Y. Evaluation of polydimethylsiloxane scaffolds with physiologically-relevant elastic moduli: interplay of substrate mechanics and surface chemistry effects on vascular smooth muscle cell response. *Biomaterials* **26**, 3123-3129 (2005).

47. Sewell-Loftin, M.K., Brown, C.B., Baldwin, H.S. & Merryman, W.D. A novel technique for quantifying mouse heart valve leaflet stiffness with atomic force microscopy. *J Heart Valve Dis* **21**, 513-520 (2012).

48. Gilbert, P.M.*, et al.* Substrate elasticity regulates skeletal muscle stem cell self-renewal in culture. *Science* **329**, 1078-1081 (2010).

49. Hsu, H.J., Lee, C.F., Locke, A., Vanderzyl, S.Q. & Kaunas, R. Stretch-induced stress fiber remodeling and the activations of JNK and ERK depend on mechanical strain rate, but not FAK. *PLoS One* **5**, e12470 (2010).

50. Burnham, K.A., D. Model Selection and Multi-Model Inference: A Practical Information-Theoretic Approach. (Springer, 2002).

51. Shi-wen, X.*, et al.* Requirement of transforming growth factor beta-activated kinase 1 for transforming growth factor beta-induced alpha-smooth muscle actin expression and extracellular matrix contraction in fibroblasts. *Arthritis Rheum* **60**, 234-241 (2009).

52. Ding, Q., Gladson, C.L., Wu, H., Hayasaka, H. & Olman, M.A. Focal adhesion kinase (FAK)-related non-kinase inhibits myofibroblast differentiation through differential MAPK activation in a FAK-dependent manner. *J Biol Chem* **283**, 26839-26849 (2008).

53. Blobe, G.C., Schiemann, W.P. & Lodish, H.F. Role of transforming growth factor beta in human disease. *N Engl J Med* **342**, 1350-1358 (2000).

54. Caraci, F.*, et al.* TGF-beta1 targets the GSK-3beta/beta-catenin pathway via ERK activation in the transition of human lung fibroblasts into myofibroblasts. *Pharmacol Res* **57**, 274-282 (2008).

55. Gu, X. & Masters, K.S. Role of the MAPK/ERK pathway in valvular interstitial cell calcification. *Am J Physiol Heart Circ Physiol* **296**, H1748-1757 (2009).

56. Walker, G.A., Masters, K.S., Shah, D.N., Anseth, K.S. & Leinwand, L.A. Valvular myofibroblast activation by transforming growth factor-beta: implications for pathological extracellular matrix remodeling in heart valve disease. *Circ Res* **95**, 253-260 (2004).

57. Hutcheson, J.D.*, et al.* Cadherin-11 regulates cell-cell tension necessary for calcific nodule formation by valvular myofibroblasts. *Arterioscler Thromb Vasc Biol* **33**, 114-120 (2013).

58. Liu, S.*, et al.* FAK is required for TGFbeta-induced JNK phosphorylation in fibroblasts: implications for acquisition of a matrix-remodeling phenotype. *Mol Biol Cell* **18**, 2169-2178 (2007).

59. Mishra, R., Zhu, L., Eckert, R.L. & Simonson, M.S. TGF-beta-regulated collagen type I accumulation: role of Src-based signals. *Am J Physiol Cell Physiol* **292**, C1361-1369 (2007).

60. Wang, Z.*, et al.* RGD-independent cell adhesion via a tissue transglutaminase-fibronectin matrix promotes fibronectin fibril deposition and requires syndecan-4/2 and {alpha}5{beta}1 integrin co-signaling. *J Biol Chem* **285**, 40212-40229 (2010).

61. Bhowmick, N.A., Zent, R., Ghiassi, M., McDonnell, M. & Moses, H.L. Integrin beta 1 signaling is necessary for transforming growth factor-beta activation of p38MAPK and epithelial plasticity. *J Biol Chem* **276**, 46707-46713 (2001).

62. Merryman, W.D.*, et al.* Correlation between heart valve interstitial cell stiffness and transvalvular pressure: implications for collagen biosynthesis. *Am J Physiol Heart Circ Physiol* **290**, H224-231 (2006).

63. Kaplan, K.B., Swedlow, J.R., Morgan, D.O. & Varmus, H.E. c-Src enhances the spreading of src-/- fibroblasts on fibronectin by a kinase-independent mechanism. *Genes Dev* **9**, 1505-1517 (1995).

64. Hinz, B., Dugina, V., Ballestrem, C., Wehrle-Haller, B. & Chaponnier, C. alpha-smooth muscle actin is crucial for focal adhesion maturation in myofibroblasts. *Molecular Biology of the Cell* **14**, 2508-2519 (2003).

65. McGarrigle, D., Shan, D., Yang, S. & Huang, X.Y. Role of tyrosine kinase Csk in G protein-coupled receptor- and receptor tyrosine kinase-induced fibroblast cell migration. *J Biol Chem* **281**, 10583-10588 (2006).

66. Playford, M.P. & Schaller, M.D. The interplay between Src and integrins in normal and tumor biology. *Oncogene* **23**, 7928-7946 (2004).

67. Pechkovsky, D.V.*, et al.* Transforming growth factor beta1 induces alphavbeta3 integrin expression in human lung fibroblasts via a beta3 integrin-, c-Src-, and p38 MAPK-dependent pathway. *J Biol Chem* **283**, 12898-12908 (2008).